Ping DSP – Evaluation of Shallow Water Bathymetry and Object Detection Capability.

Sebastian Senyo BOTSYO, Ghana, Timothy SCOTT, Kenneth KINGSTON and Adam BOLTON, United Kingdom

Faculty of Science and Engineering, School of Biological and Marine Sciences, University of Plymouth, United Kingdom.

SUMMARY

This paper evaluates the performance of the Ping DSP's 3DSS-IDX-450 sonar in shallow water surveys, comparing it against traditional multibeam echo sounders (MBES) like the Norbit iWBMS. The study assessed bathymetric uncertainty and object detection capabilities according to the International Hydrographic Organization (IHO) standards. The research was conducted in Cawsand Bay, employing both the 3DSS-IDX-450 sonar and the Norbit iWBMS to collect bathymetric data and detect objects on the seabed and mid-water. Data processing and analysis were performed using software like QPS Qimera and CloudCompare, focusing on bathymetric performance and object detection. Results indicated that the 3DSS-IDX-450 sonar provides bathymetric soundings comparable to traditional MBES systems. The overall depth uncertainty for Norbit iWBMS was 0.042m and 0.11m (95% c.l.) for 3DSS-IDX-450. It successfully detected objects both on the seabed and mid-water, demonstrating its efficiency in identifying targets with its Computed Angle-of-Arrival Transient Imaging (CAATI) technology. The sonar's performance in shallow water met IHO Order 1a and 1b, making it suitable for various applications, including naval and autonomous surface vehicle (ASV) operations. The study concludes that the 3DSS-IDX-450 sonar is a reliable tool for shallow water hydrographic surveys, offering advantages in terms of size, power consumption, and integrated technologies for challenging environments.

Key words: Bathymetry, CAATI, interferometry, backscatter, object detection.

PING DSP – Evaluation of Shallow Water Bathymetry and Object Detection Capability

Sebastian Senyo BOTSYO, Ghana, Timothy SCOTT, Kenneth KINGSTON and Adam BOLTON, United Kingdom

Faculty of Science and Engineering, School of Biological and Marine Sciences, University of Plymouth, United Kingdom.

1.0 Introduction

The increasing demand for effective, efficient, and accurate instrumentation and technologies for hydrographic surveying has influenced the adoption of disruptive techniques and solutions that impact survey capacity and productivity. In hydrographic surveying, whether underwater acoustic sensor measurements or underwater positioning, the quality of the sensed data is crucial (Crawford and Connors, 2019) for sediment categorisation, underwater topography, and geomorphology analysis (Bu *et al.*, 2021; Kenny *et al.*, 2003). Several applications of hydrography (e,g, wrecks and underwater archaeology, surveying subsea structures, shallow water hydrography, Autonomous Surface Vehicles (ASV) and Autonomous Underwater Vehicles (AUV) applications) (Geen, 1998) are making use of the combination of side-scan sonar (SSS) and multibeam echosounder (MBES) as separate systems for data acquisition and analyses (Fakiris et al., 2019; Shang *et al.*, 2019). However, with the advent of recent technologies, interferometric sonars like Ping Digital Signal Processing (DSP) have been developed to combine MBES and SSS capability systems for underwater imaging and mapping. This system integrates side-scan, IHO Exclusive Order swath bathymetry, and 3D point clouds as one single system. The Ping DSP has real-time 3DSS™ high-definition imaging technology and MBES Bathymetry Engine and is designed to work on a range of Automated Surface and Underwater Vehicles. The 3DSS™ introduces accurate three-dimensional side-scan imaging and extends the swath bathymetry side-scan beyond traditional interferometry's inherent limitations. 3DSS™ explicitly resolves multiple instantaneous angles of arrival. It separates seabed backscatter from the sea surface, water column and multipath backscatter (Ping DSP Inc, 2018b) – something traditional interferometric swath sounders had been unable to achieve. The Ping DSP is designed for shallow water surveys and provides comprehensive bathymetric coverage of the seabed, even at nadir (Brisson *et al.*, 2014) with its Computed Angle-of-Arrival Transient Imaging (CAATI) algorithm. The Ping DSP capabilities stated have been evaluated in a robust performance assessment against the International Hydrographic Organization (IHO) standards (IHO, 2020). The IHO requirements define strict standards applicable to hydrographic surveys worldwide. Existing literature (e.g., Kraeutner *et al.*, 2002; Crawford and Connors, 2019) attempted to assess the performance the earlier model (3DSS-DX-450) of the Ping DSP under different scenarios of what is presented in this paper. The study explored some practical applications of the 3DSS-IDX-450 with survey operations performed at Cawsand Bay. The Ping DSP sonar was mobilised on an Unmanned Surface Vehicle (USV), the Yellow Pig due to the short length of its sonar cable (1.5m) which was not suitable for deployment on a manned vessel, while the Norbit iWBMS was deployed on a manned vessel, Falcon Spirit. Even though the setup, geometry and operational requirements of the systems were different, the survey

operations and data acquisition procedures were as similar to each other as possible. The 3D data of soundings captured contributed to comparisons with the Norbit iWBMS multibeam, offering an insight into its functionalities. After post-processing, the 3D data can be used as backscatter seabed imagery, bathymetry, or a combination of the two. However, the several tests performed with the 3DSS-IDX-450 sonar and the Norbit iWBMS focused on the bathymetric accuracy and object detection capability with surveys over seabed and mid-water targets. This paper also discusses the technological advancements represented by the Ping DSP's 3DSS-IDX-450.

2.0 Materials and Methods

2.1 3DSS-IDX-450 – Description and Operational requirements

The 3DSS-IDX-450 (Figure 1) is a shallow water mapping and imaging sonar integrated with AML MicroX Sound Velocity Sensor, SBG Ellipse2-E IMU and Septentrio dual GNSS for superior hydrographic survey performance. The 3DSS-IDX-450 features a patented signal processing approach that extends the single angle-of-arrival principle used in interferometric systems to accommodate multiple simultaneous backscatter arrivals. The Sonar operates at 450 kHz and consumes a maximum power of 22W and voltage requirements of 24VDC ±10%. The dimensions of the Sonar are 56.8 cm (length) x 9.8 cm (diameter), 10m depth rating, and it weighs 8kg in air. It operates with a horizontal beamwidth (2-way) of 0.4º and vertical beamwidth (selectable) of 15º – 125º with 1440 soundings per Ping across the swath at a ping rate of 30Hz. The integrated MRU have an accuracy of 0.5º for roll and pitch with an external input interface of 1PPS, RS-232, NMEA and TTS protocols (Ping DSP Inc., 2020). Table 1 contains the key system specifications for 3DSS-IDX-450 Sonar.

Figure 1. (A) 3DSS-IDX-450 Sonar with GNSS. (B) Sonar Interface Unit (SIU) powers the sonar head and has an integrated

Ethernet switch for communication with the sonar head (Ping DSP Inc., 2021).

2.2 Norbit iWBMS – Description and Operational requirements

The Norbit iWBMS MBES system with embedded Applanix WaveMaster II was over-the-side mounted on a pole attached to a frame on Falcon Spirit with the transducer connected to a flange with locking nuts, reducing vibration (Figure 2). For good connections between the equipment, programs and regular collection, a test was done to assess communication between the Norbit iWBMS, the Sonar Interface Module (SIM) and the Norbit data acquisition software.

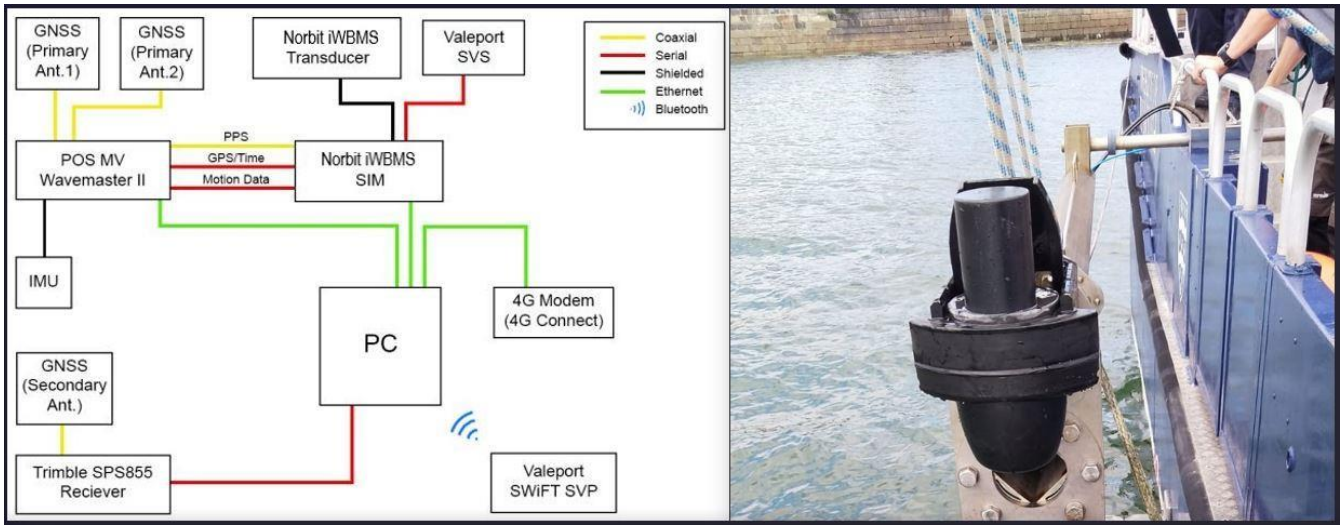

Figure 2. Data and communication configuration for Norbit iWBMS (left) and the vessel mount (right)

2.3 Mobilising Yellow Pig with the 3DSS-IDX-450 Sonar

The mobilisation of the Yellow Pig with the 3DSS-IDX-450 side scan sonar system involved the physical installation of devices and electrical and electronic connections with operational data collection and navigation software (Qinsy and 3DSS-DX Control). The Sonar was installed using its pole adaptor onto a 1m pole (5cm in diameter). The pole was 1m from the mounting adapter to the top of the T-piece to the flange. Two GNSS antennas (primary and secondary) were fitted 2m apart on the T-piece bar and connected to ANT1 and ANT2 on the topside box (SIU). The 3DSS-IDX-450 was moon pool mounted on the Yellow Pig 30cm below the water surface to minimise the possibility of a secondary transmit pulse resulting from surface bounce multipath due to the proximity of a strong reflector above the Sonar (Leenhardt, 1974). A pelican case containing the integrated SIU with a laptop, GNSS receiver, smartphone and 300W power source was connected using the 3DSS^{TM}-DX sonar cable (1.5m long with Teledyne Impulse MHDG-CCP-16 underwater connector that mates with the MHDG-FCR-16 on the Sonar) to power the sonar head. The 3DSS-IDX-450 system operated independently of the Yellow Pig. The GNSS antenna offsets were programmed into the Ellipse-2 INS through the 3DSS Control Console interface. Figure 3 shows the setup on the Yellow Pig with the 3DSS-IDX-450 Sonar.

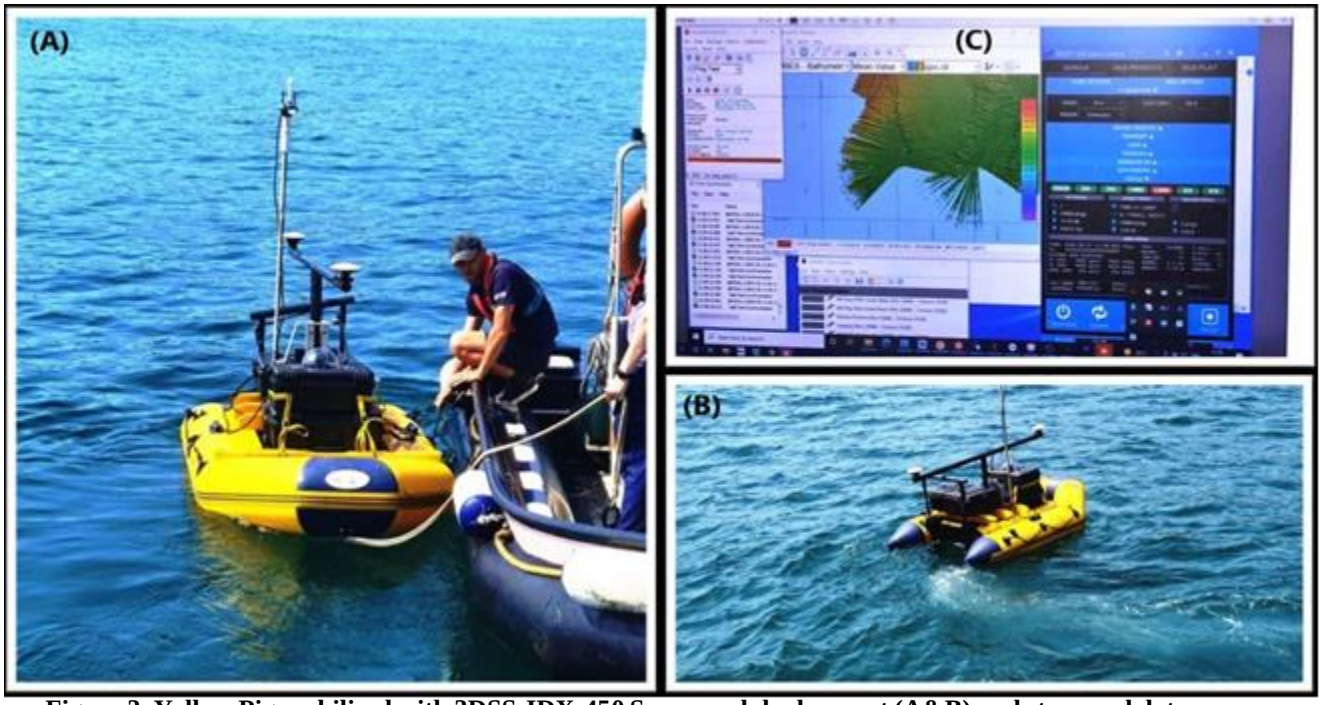

Figure 3. Yellow Pig mobilised with 3DSS-IDX-450 Sonar and deployment (A&B) and streamed data visualisation (C).

Table 1. Key system specifications for 3DSS-IDX-450 Sonar.

System Features	Specifications
Operating Frequency	450kHz
Horizontal Beamwidth (2-way)	0.4º
Vertical Beamwidth (selectable)	15º - 125º
Number of Beams	512
Mech. Transducer Tilt (fixed)	20º
Electronic Transmit Tilt	-45º to 45º
Max. Ping Rep. Rate	~30Hz
Data Output	Rage, Angle, and Amplitude (2D & 3D)
Max. Range	2D 200m per side and 3D 100m per side
Max. Resolution	1.67cm
Typical Bathymetry Swath Width	6 to 14 times sonar altitude, varies with sound velocity profile and bottom type
Roll and Pitch	0.5º
Depth Rating	10m

2.4 Testing Location: Cawsand Bay

Cawsand Bay is located on the southeast coast of Cornwall and about 5km southwest of Plymouth Sound (Saunders *et al.*, 2003) (Figure 4). Several high levels of scientific and academic research (e.g. Gibbs, 1969; Dando, 1975; Kendall and Widdicombe, 1999; Parry *et al.*, 1999) have been conducted in Cawsand Bay owing to its shallow seabed with a steady slope to death of 10m below chart datum, sediment composition (a mixture of mud, fine sand and tiny shells in deeper waters, and sand nearer inshore) and different marine species (Gibbs, 1969).

The Cawsand Bay (5-10m CD) testing site within Plymouth Sound was selected. The area was chosen because its shallow nature suited the 3DSS-IDX-450 Sonar, designed for shallow water depth surveys, and deployed on USV (Yellow Pig). USV operations are also limited to certain areas within.
the Dockyard limits (Cawsand Bay and immediately south of the Plymouth breakwater) in Plymouth Sound. The deployment location has a 0.5m calibrated cube suitable for testing seabed object detection capabilities of acoustic sonars per IHO Standards. It is also a designated area with structured survey lines for reference surface analysis due to its gradual depth slope in shallow water.

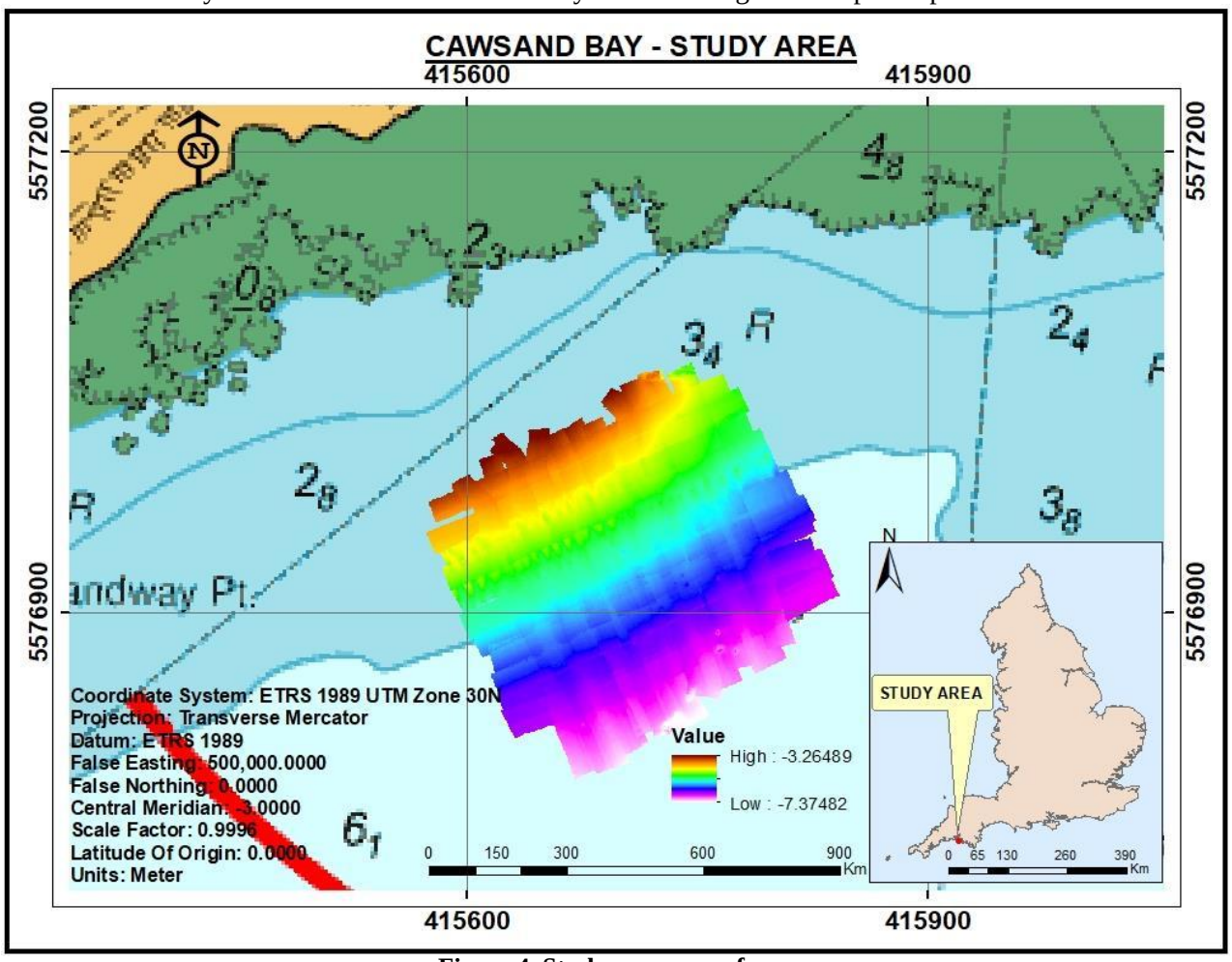

Figure 4. Study area map of Cawsand Bay

3.0 Data Collection

The Norbit MBES bathymetric and object detection data collection was conducted on Monday 13th June 2022, at Cawsand Bay from 09:25 to 14:20 British Summer Time (BST) using the Falcon Spirit survey vessel, and that of the 3DSS-IDX-450 Sonar was performed on Friday 17th June 2022 from 10:00 to 15:00 BST using the Yellow Pig USV. The geodetic datum and projection parameters used for the survey, data processing and bathymetric map were ETRS89_UTM_Zone_30N (GRS'80 Spheroid) with metres as the unit of measurement. The survey vessel (Falcon Spirit) for the Norbit MBES survey was mobilised the week before the day of the survey. Vessel speed was controlled to maintain data quality, and line spacing was designed to achieve 100% overlap between lines. The quality of the multibeam data was monitored in real time during the data collection. The weather was assessed to ensure wind speed and force did not impact the capability of the Yellow Pig to follow and trace the pre-defined survey lines. The weather conditions were generally favourable (calm and flat sea) for the data collection on both days. The area cellular (4G connectivity) was monitored for possible outages since it would determine the ability to operate the Yellow Pig remotely.

3.1 Bathymetric Uncertainty Test (Reference Surface) - Norbit iWBMS and 3DSS-IDX-450 Sonar

Line planning was done using the QPS Quality Integrated Navigation System (QINSy) hydrographic survey software and Mission Planner (for the Yellow Pig USV). The survey grid lines (orthogonal – East- West and South-Nouth) were 15m apart, allowing for 100% overlap (Figure 5). The length of the survey lines was 150m—the survey grid lines perpendicular to shore and shore parallel for cross-checking were surveyed using the Norbit iWBMS with an average vessel speed of 5 knots. The Norbit iWBMS multibeam operated with a frequency of 400kHz, 110º swath coverage (beam angle) with 256 beams (equidistant). The East-West and South-North method of reference surface survey provided heavy overlaps at the nadir with no beam preference over the surface. They indicated beam homogeneity across the surface regarding the beam angle used in each beam. The sound velocity profiles were taken using a Valeport SWiFT SVP at the start, during and before the end of the survey. The SVP data was downloaded and applied in Qinsy through a Bluetooth connection to correct data for sound velocity. Applanix POS MV Wavemaster II, Trimble SPS855 with NTRIP RTK and CNAV300 with PPP corrections provided horizontal and vertical positions for the survey. All soundings were reduced to Chart Datum using dual-frequency carrier-phase GNSS height observations combined with the UKHO VORF model. Soundings are presented as depths below Chart Datum using 49.076m VORF correction.

3DSS-IDX-450 Sonar aboard the Yellow Pig surveyed the same area as the Norbit MBES but with 25m line spacing at an average speed of 2 knots with 450kHz, 37m range (i.e.,160º beam angle at 6.5m water depth, and filtered at 142º), 0.5º beamwidth and 512 beams. The length of the survey lines was 150m. The Yellow Pig was programmed to follow the pre-defined survey lines autonomously with monitoring from the control station on the support vessel. The First-Person View (FPV) camera provided images of navigation. The autopilot controls were interfaced through a standard R.C. control system. In situations where the Yellow Pig lost a 4G connection for the autopilot, the system was controlled using the Mission Planner software and the ardupilot flight control system configured as a

ground rover. Line selection and data logging was performed in Qinsy on the support vessel. The data was stored on the host computer and streamed to the client computer on the support vessel (Figure 3 C). Positioning was provided by the 3DSS-IDX-450 Sonar integrated SBG INS/GNSS receiving RTK corrections from Plymouth University's GNSS base station at the Marine Station via a 4G network connection.

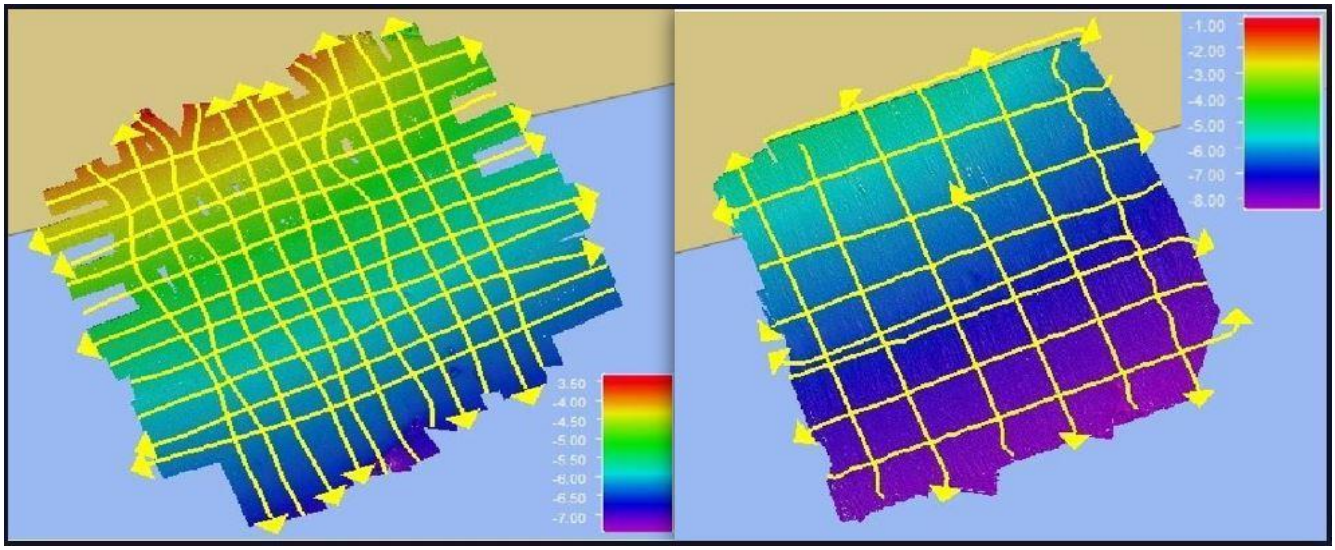

Figure 5. The Norbit iWBMS (left) and 3DSS-IDX-450 (right) surveyed reference surface grid lines.

3.2 Bathymetric Uncertainty Test (Star Patten) – Norbit iWBMS & 3DSS-IDX-450 Sonar

Data for the bathymetric uncertainty tests was collected using 'star pattern' lines (Figure 6) across the high-resolution reference area to minimise the impact of wave motion on the dataset. Each line was surveyed twice in reciprocal directions at the same survey speed as much as possible. The lines were run so that the sonar head passed the same area on each run. The lines were run at 400kHz, 256 beams with 160º swath angle (equiangular) for the Norbit iWBMS and 450 kHz, 512 beams and 37m range per side for the 3DSS-IDX-450 Sonar. The star pattern data was used with the reference

surface data to determine the bathymetric uncertainty associated with the performance of both systems.

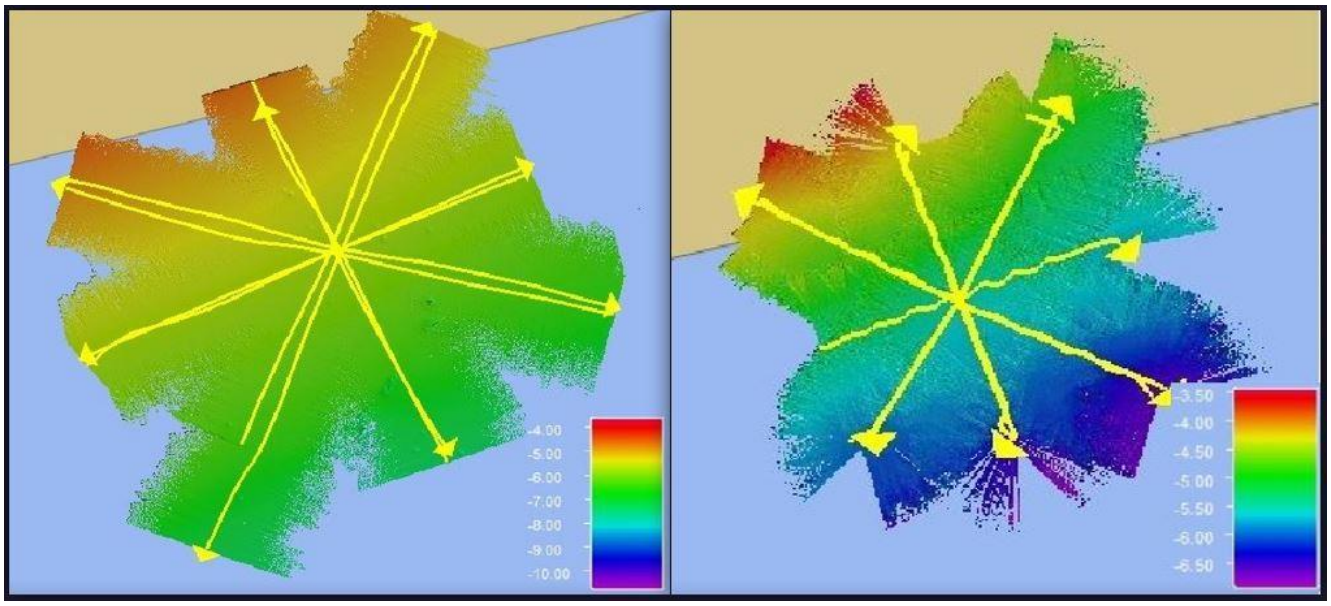

Figure 6. Star Pattern Survey of Norbit iWBMS (left) & 3DSS-IDX-450 Sonar (right).

3.3 Object Detection (Norbit iWBMS & 3DSS-IDX-450) – a seabed and mid-water target

The object detection survey was planned around a pre-calibrated 0.5m cubic seabed target in Cawsand Bay. A circular midwater object (0.65m in circumference) was also placed within a 15m radius of the cube at about 3m depth (Figure 7). The cube was centred using the coordinate of its location obtained at the time of placement. Two squares (survey lines) with distances of 10m and 20m measured from the cube's centre (at 0m) were drawn around the cube. This is to test the ability of both sonars to detect the object at the nadir (0º-20º), 10m (mid-swath 30º-60º) and 20m (outer swath 70º-80º) away from the object. Each line (over the target, 10m and 20m apart) was surveyed twice in reciprocal directions (port and starboard) at the same surveying speed as possible.

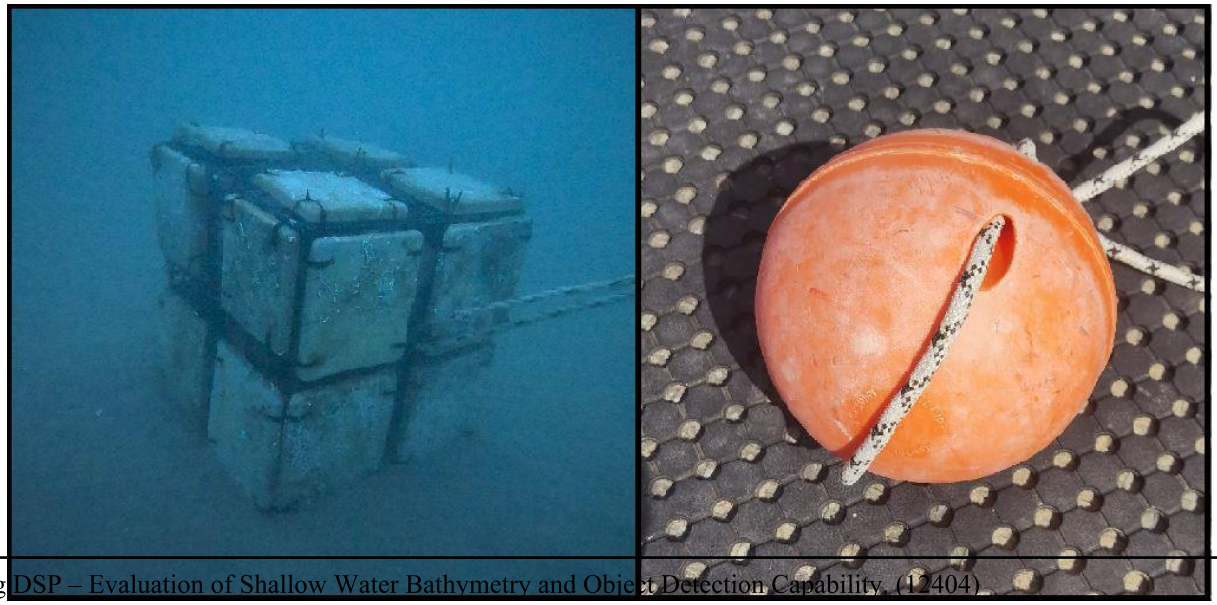

Figure 7. 0.5m Seabed target (left) and 0.65m midwater target (right)

3.4 Data Processing

The raw sonar files for both Norbit iWBMS and 3DSS-IDX-450 were processed in QPS Qimera software. The data were thoroughly examined and grouped into reference surface, star pattern and object detection to make them easy to process. Dynamic surfaces for each grouping were created with 0.25m resolution. VORF correction of 49.076m of the study area was applied to reduce all soundings to Chart Datum. The position and navigation data stored in each file were verified, and erroneous soundings were cleaned with the 2D and 3D editors. Ten separate calibration computations were performed to derive a standard deviation that indicated the accuracy of the derived values of the roll, pitch and heading (yaw). The entire MBES data for both systems were generally less noisy due to the adherence to quality control measures (online Q.C., online logs, data quality verification etc.) used during the data collection. However, the 3D side scan data of the 3DSS-IDX-450 Sonar was very noisy because of its ability to collect water column data. The data was cleaned manually not to delete possible data using the algorithm cleaning tools. The Cross Check Tool in QPS Qimera software was used to conduct a crossline analysis of the collected data to measure the reliability of the multibeam data collected during the survey. The reference surface data and the star pattern lines were used in the analysis.

Dynamic surfaces of 0.25m resolution were created for each of the object detection lines (over the top of cube 0m, 10m and 20m offsets) and the combined lines to determine the number of hits from each passage. The cube was identified in the MBES data of both sonars but not in the 3DSS data. The midwater target was captured in the MBES and 3DSS data of the 3DSS-IDX-450 Sonar but not in the Norbit data.

4.0 Results

4.1 Bathymetry Uncertainty Test

The purpose of the reference surface analysis was to make a measured assessment of the uncertainty on the day of the survey. This analysis provided a high level of confidence in the data quality and the performance of the systems. The orthogonal lines indicated heavy overlaps of soundings with homogeneous beams across the surface concerning the beam angle used in each beam. The crosslines (star pattern lines) represented the setup used for the survey with a full swath width. Every ping from the crosslines was compared to the reference surface depth. The star pattern lines ran from every direction, provided average depth uncertainty to minimise bias from wave motion and other systematic errors. Statistical assessment of the errors across the crosslines and overall estimation of the difference between the sounding on the crosslines and the underlying reference surface aided the computation of uncertainty estimates for a 95% confidence level. In figure 10
the bathymetric performance of both systems per IHO Order 1 and Special Order are shown. System performance comparative plots based on the Depth Uncertainty (in metres, 95% c.l.) plus absolute Mean Bias (m) against the beam angle indicated both systems achieved the standard of IHO Order 1a for bathymetric uncertainty (figure 8). However, the 3DSS-IDX-450 performed comparatively less accurate at the nadir, as shown in Figures 8 & 9. The error of the nadir performance of the 3DSS-IDX-450 was 0.428m (M.B. data) and 0.513m (3D data) compared to 0.306m of the Norbit iWBMS at its nadir. Figure 9 presents the bathymetric performance of both systems per the IHO Special Order. The 3DSS-IDX-450 did not meet the overall IHO Special Order because its bathymetric ability deteriorated quickly with high uncertainty on the outer beams above 140º (32m range) in shallow water. It, however, performed better in the middle from 20º-140º. The Norbit iWBMS performed better in the outer beams, up to about 155º. The overall depth uncertainty for Norbit iWBMS was 0.042m and 0.11m (95% c.l.) for 3DSS-IDX-450. The cross-check statistics are displayed in figure 10.

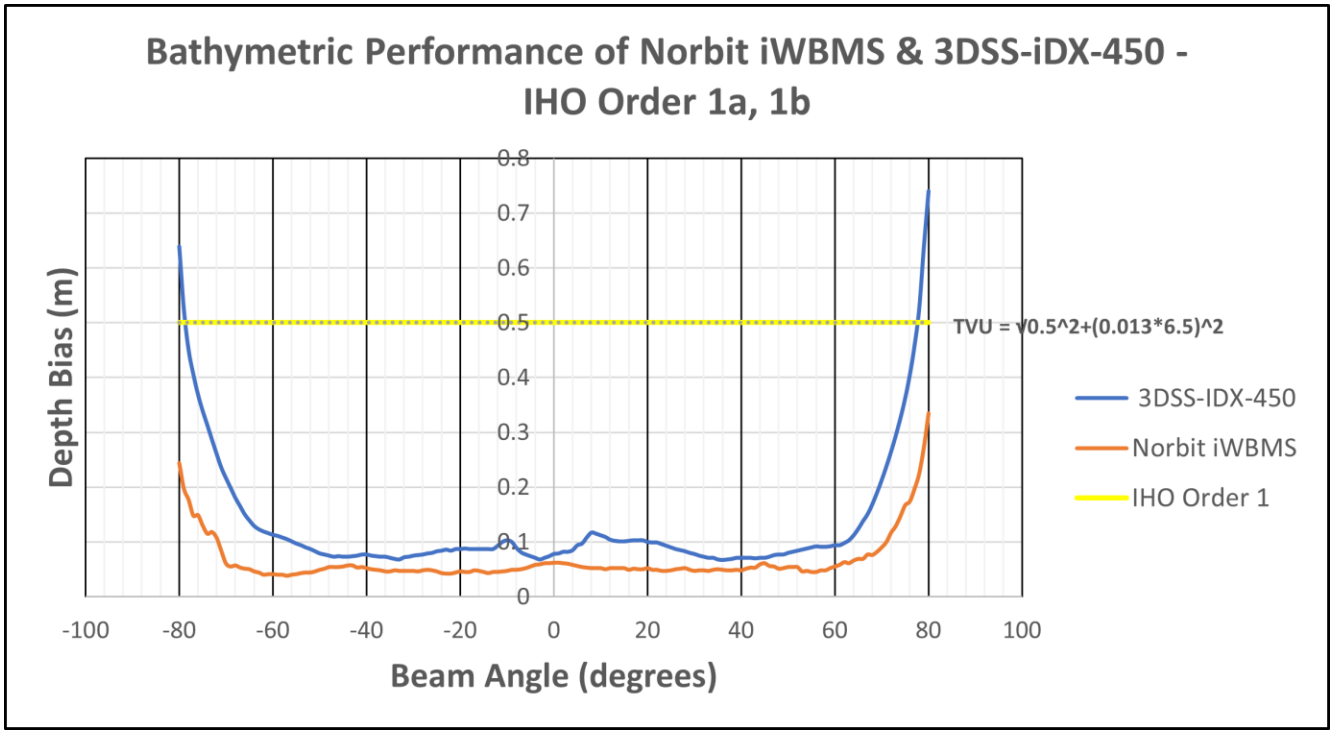

Figure 8. Plot showing bathymetric performance of both systems per IHO Order 1.

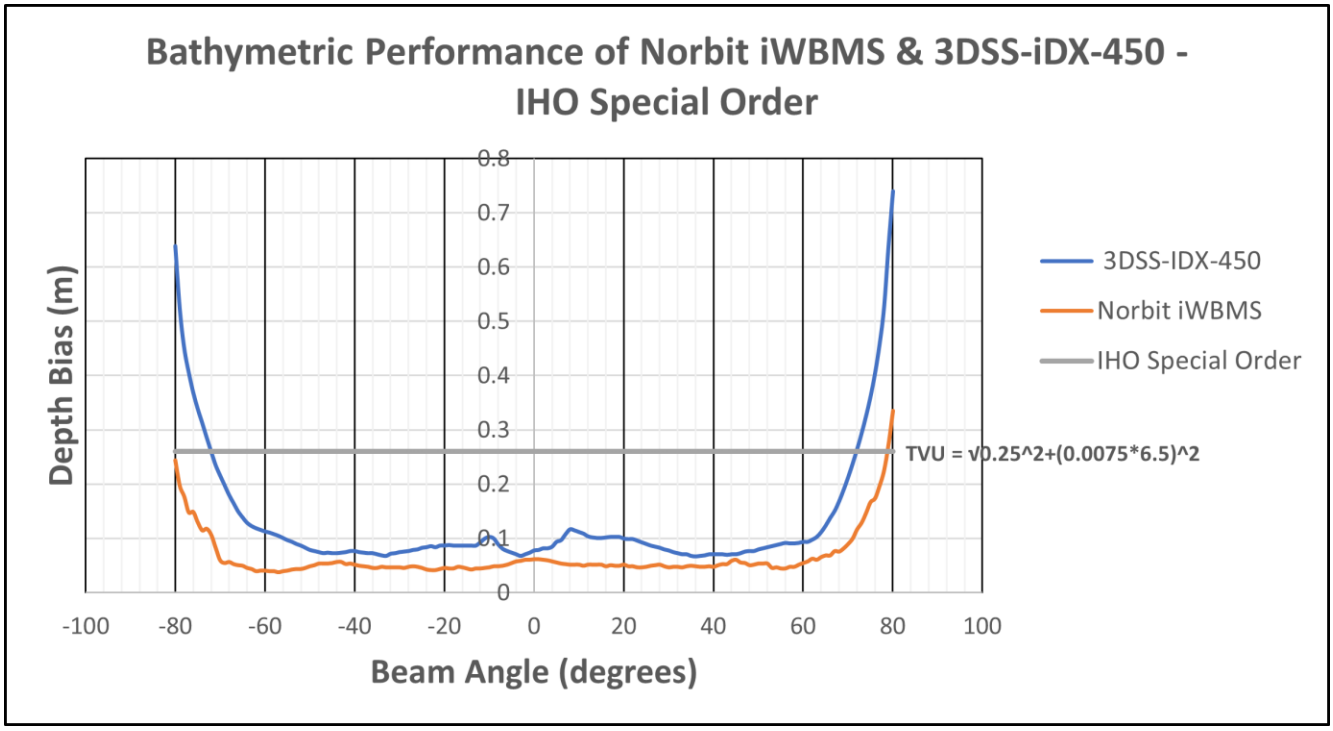

Figure 9. Plot showing bathymetric performance of both systems per IHO Special Order.

IHO Order 1 Statistics

Norbit iWBMS

Statistic	Value
Order 1 Error Limit	0.504947
Order 1 # Rejected	179
Order 1 P-Statistic	7.31914e-05
Order 1 Test	ACCEPTED
Number Of Points	2445643
Grid Cell Size	0.250
Difference Mean	0.011
Difference Median	0.010
Difference Std. Dev	0.034
Difference Range	[-1.159, 1.180]
Mean + 2*Stddev	0.078
Median + 2*Stddev	0.077
Data Mean	-5.413
Reference Mean	-5.424
Data Z-Range	[-7.406, -3.389]
Reference Z-Range	[-7.433, -3.637]

3DSS-IDX-450

Statistic	Value
Order 1 Error Limit	0.504903
Order 1 # Rejected	108466
Order 1 P-Statistic	0.0180014
Order 1 Test	ACCEPTED
Number Of Points	6025422
Grid Cell Size	0.500
Difference Mean	0.119
Difference Median	0.080
Difference Std. Dev	0.139
Difference Range	[-2.038, 1.994]
Mean + 2*Stddev	0.397
Median + 2*Stddev	0.358
Data Mean	-5.280
Reference Mean	-5.400
Data Z-Range	[-8.472, -3.043]
Reference Z-Range	[-6.768, -3.606]

IHO Special Order Statistics

Norbit IWBMS

Statistic	Value
Special Order Error Limit	0.253288
Special Order # Rejected	2704
Special Order P-Statistic	0.00110564
Special Order Test	ACCEPTED
Number Of Points	2445643
Grid Cell Size	0.250
Difference Mean	0.011
Difference Median	0.010
Difference Std. Dev	0.034
Difference Range	[-1.159, 1.180]
Mean + 2*Stddev	0.078
Median + 2*Stddev	0.077
Data Mean	-5.413
Reference Mean	-5.424
Data Z-Range	[-7.406, -3.389]
Reference Z-Range	[-7.433, -3.637]

3DSS-IDX-450

Statistic	Value
Special Order Error Limit	0.253259
Special Order # Rejected	949034
Special Order P-Statistic	0.157505
Special Order Test	REJECTED
Number Of Points	6025422
Grid Cell Size	0.500
Difference Mean	0.119
Difference Median	0.080
Difference Std. Dev	0.139
Difference Range	[-2.038, 1.994]
Mean + 2*Stddev	0.397
Median + 2*Stddev	0.358
Data Mean	-5.280
Reference Mean	-5.400
Data Z-Range	[-8.472, -3.043]
Reference Z-Range	[-6.768, -3.606]

Figure 10. Cross Check Statistics generated in Qimera for both systems per IHO Order 1 and Special Order.

4.2 Object Detection (Bathymetric Repeatability)

The bathymetric repeatability was done to evaluate the ability of the sonars to hit the object in the same place from different angles. The test monitored the three-dimensional positions of a pre-calibrated 0.5m detectable cube on the seabed and a 0.65m midwater target within a 15m radius of the cube at Cawsand Bay. The features were surveyed first at the nadir from multiple directions (north, south, east, and west). Secondly, the targets were boxed-in so that they appeared in the outer beams on the port for two lines (10m and 20m offsets from the object) and the outer beams on the starboard for two lines. The computed statistical reliability of the horizontal position and the depth measured for the targets are shown in table 2 and table 3. The average coordinates of cube location from all angles and their deviational accuracies from the known coordinate are shown in table 4.

Table 2. Summary Statistics of hits on the target by Norbit iWBMS.

NORBIT	**Nadir (0m - Over Target)**			**10m offsets**			**20m offsets**		
Elements	E	N	Z	E	N	Z	E	N	Z
Average	415702.162	5576939.741	-5.218	415702.098	5576939.641	-5.211	415702.096	5576939.583	-5.221
StdDev	0.276	0.357	0.095	0.224	0.390	0.079	0.276	0.293	0.121
Minimum	415701.648	5576939.202	-5.543	415701.611	5576939.04	-5.517	415701.504	5576939.012	-5.499
Maximum	415702.92	5576940.442	-5.047	415702.704	5576940.488	-4.989	415702.887	5576940.229	-4.969
Total Hits	**178**			**291**			**130**		

Table 3. Summary statistics of hits on the target by 3DSS-IDX-450.

3DSS-IDX-	**Nadir (0m - Over Target) - 3D**			**10m offsets - 3D**			**20m offsets - 3D**		
Elements	E	N	Z	E	N	Z	No hits		
Average	415702.417	5576939.701	-5.0998	415702.164	5576940.128	-5.412			
StdDev	0.348	0.320	0.089	0.240	0.368	0.171			
Minimum	415701.536	5576938.921	-5.594	415701.725	5576939.08	-5.641			
Maximum	415702.346	5576940.592	-4.905	415702.769	5576940.477	-5.006			
Total Hits	**83**			**861**					
3DSS-IDX-	**Nadir (0m - Over Target) - MB**			**10m offsets - MB**			**20m offsets - MB**		
Elements	E	N	Z	E	N	Z	E	N	Z
Average	415702.385	5576939.812	-5.214	415702.163	5576939.947	-5.391	415702.054	5576939.991	-5.390
StdDev	0.381	0.322	0.064	0.287	0.362	0.145	0.264	0.299	0.151
Minimum	415701.631	5576939.253	-5.34	415701.5	5576939.164	-5.677	415701.502	5576939.5	-5.594
Maximum	415702.581	5576940.42	-5.083	415702.45	5576940.102	-5.103	415702.543	5576940.738	-5.072
Total Hits	**61**			**334**			**205**		

Table 4. Average coordinates of cube location from all angles and their deviational accuracies from the known coordinate.

Components	Em	Nm
Known Coord. (A)	415702.000	5576940
Norbit 0m (B)	415702.162	5576939.741
Norbit 10m (C)	415702.098	5576939.641
Norbit 20m (D)	415702.096	5576939.583
3DSS 0m -3D (E)	415702.417	5576939.701
3DSS 10m -3D (F)	415702.164	5576940.128
3DSS 0m -MB (G)	415702.385	5576939.812
3DSS 10m -MB (H)	415702.163	5576939.947
3DSS 20m -MB (I)	415702.054	5576939.991
	ΔEm	**ΔNm**
Norbit 0m (A-B)	-0.162	0.260
Norbit 10m (A-C)	-0.098	0.359
Norbit 20m (A-D)	-0.096	0.417
3DSS 0m -3D (A-E)	-0.417	0.299
3DSS 10m -3D (A-F)	-0.164	-0.128
3DSS 0m -MB (A-G)	-0.385	0.188
3DSS 10m -MB (A-	-0.163	0.053
3DSS 20m -MB (A-	-0.054	0.009

4.3 Seabed Target

The Norbit iWBMS and 3DSS-IDX-450 had hits on the seabed target (0.5m cube) at the nadir, 60º (10m offsets around the cube) and 70º (20m offsets). The accuracies of the sonars in hitting the target based on the given coordinate of the cube are indicated in table 5. Figure 11 shows how each sensor identified the target.

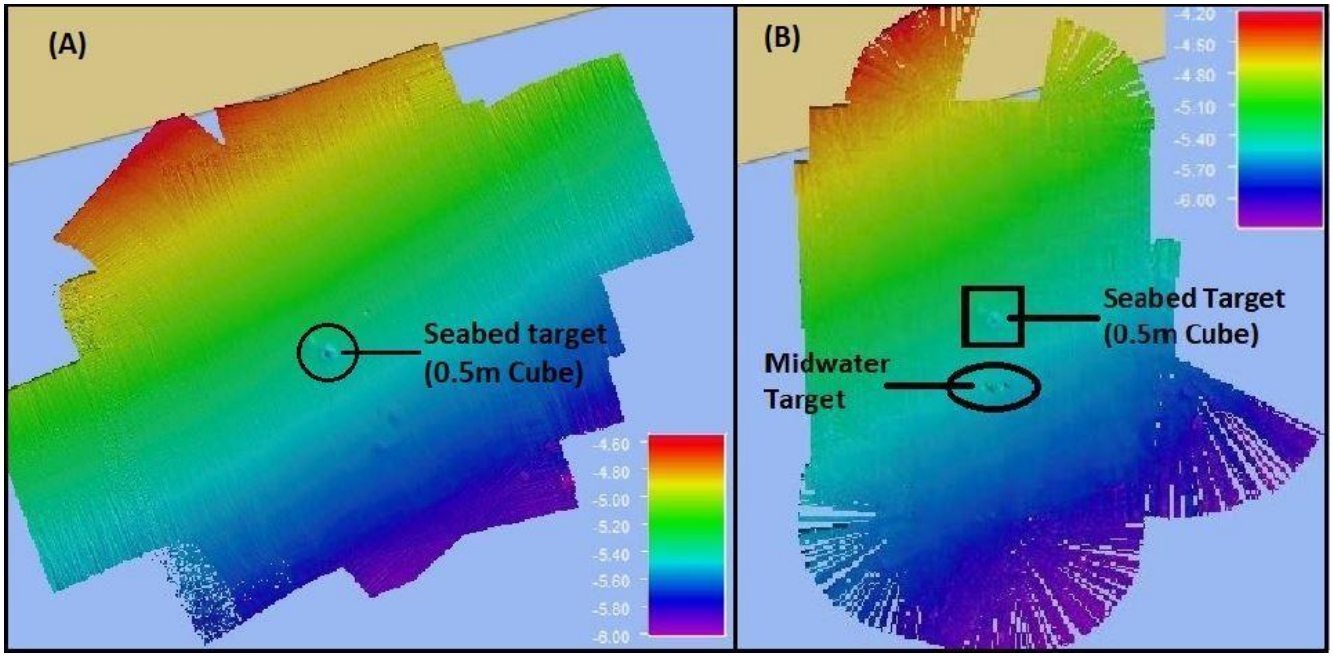

Figure 11. Seabed and mid-water targets as surveyed by both sonars – Norbit (A) and 3DSS-IDX (B)

Table 5. Accuracy of hits on target.

Sonar	E (95% CL)	N (95% CL)
Norbit iWBMS	0.029 m	0.062 m
3DSS-IDX-450 3D	0.120 m	0.203 m
3DSS-IDX-450 MB	0.103 m	0.072 m

The 3DSS-IDX-450 signal processing and sonar array have augmented the CAATI approach to generate 3D point cloud data. Figure 12 shows samples of images showing the 0.5m cube seafloor target imaged by the Norbit and 3DSS-IDX-450 sonars as multibeam and 3DSS point cloud, with the colours of the points scaled by backscatter intensity.

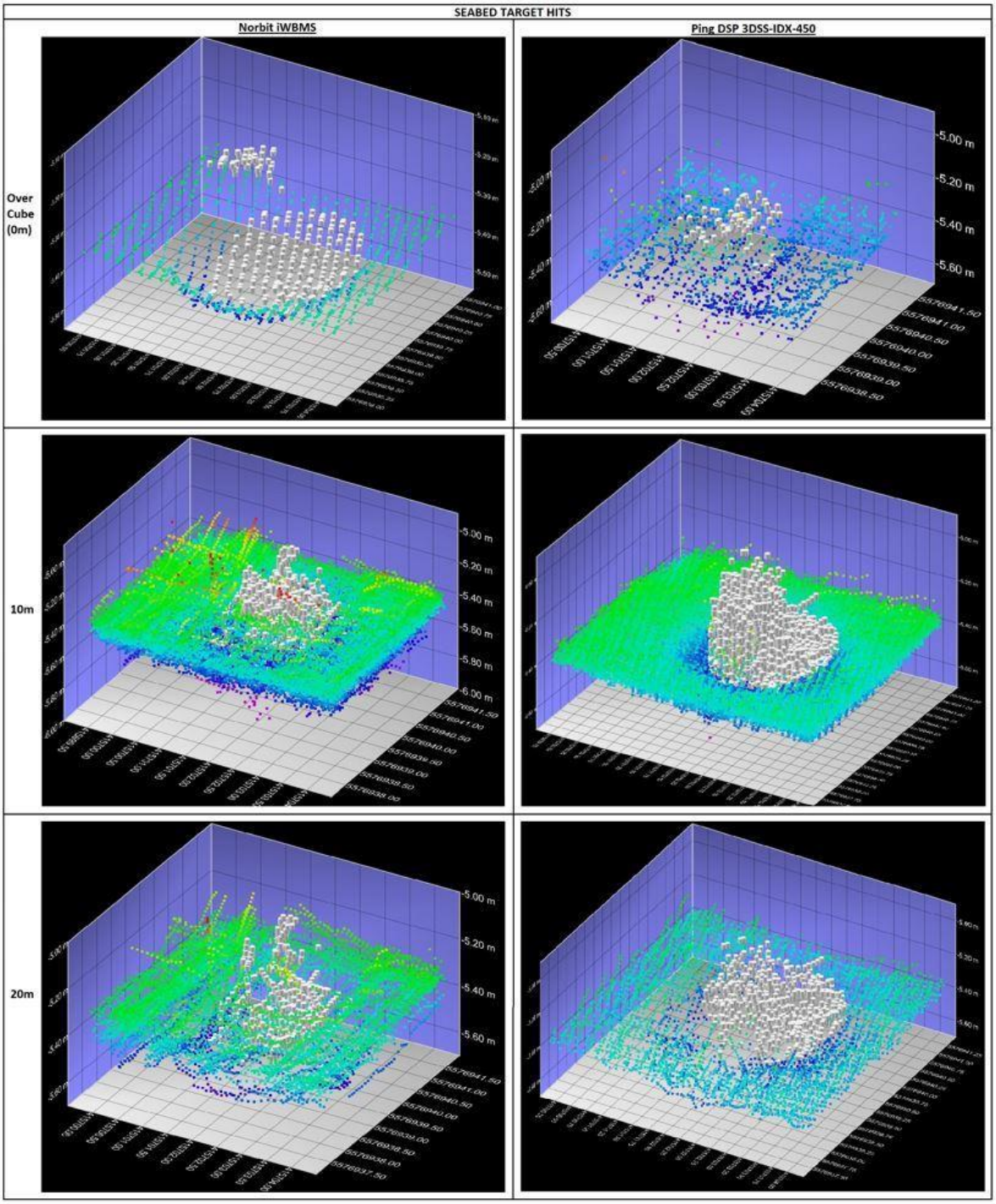

Figure 12. Sampled images of the 0.5m cube seafloor target imaged from all angles representing 0m, 10m and 20m distances

4.4 Mid-water Target

The key objective of the test was to evaluate the performance of the 3D side scan sonar in detecting moored objects in mid-water. The target, including the tethering cable and the seabed anchor, were recognisable from the acoustic signal returns from the water column. The point cloud from the passes by the 0.65m sphere extracted for assessment is shown in figures 13 & 14. The intensity of the backscattered signal highlighted the spherical nature of the object. The mid-water target could not be identified in the Norbit data.

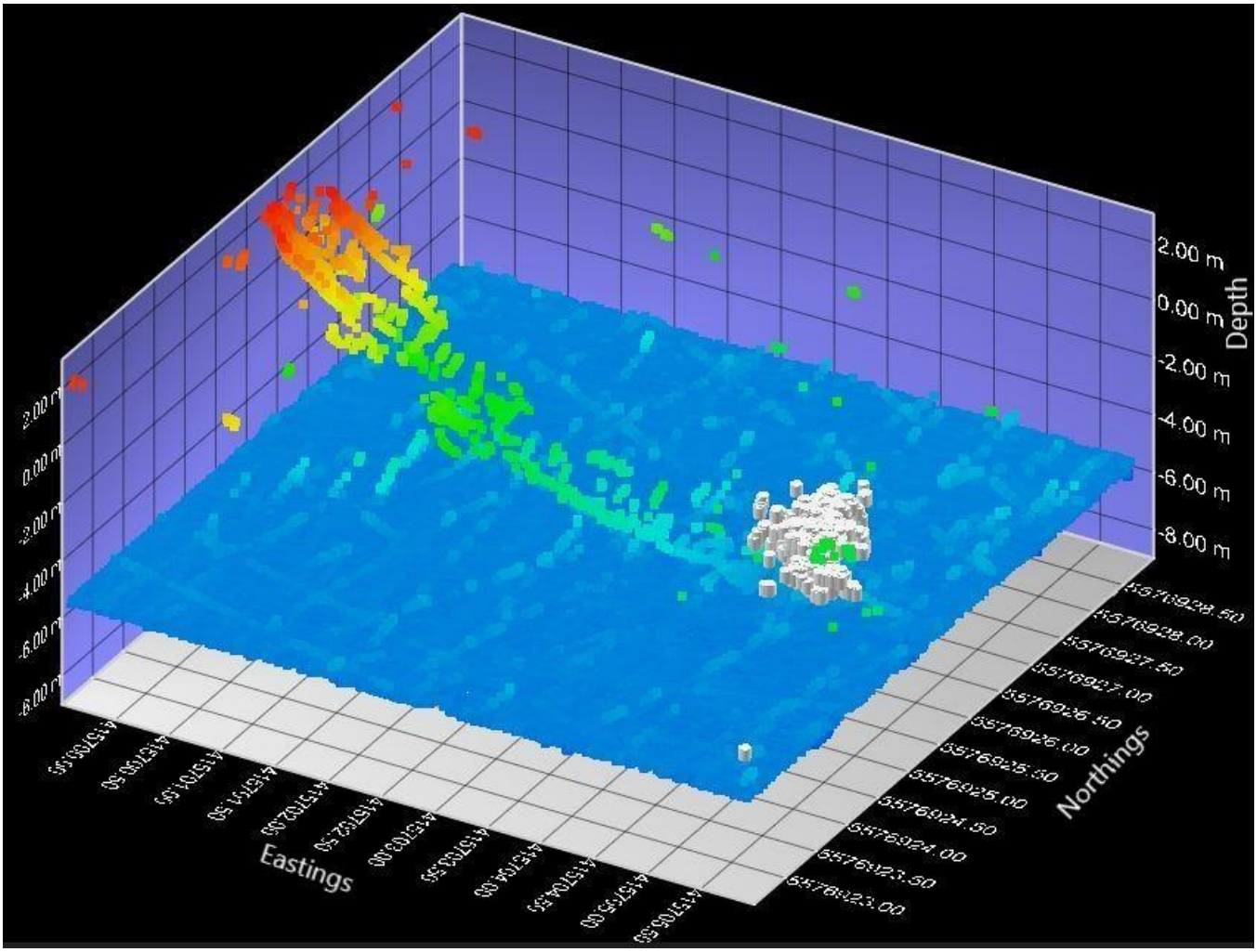

Figure 13. 3D Side Scan data of the mid-water target.

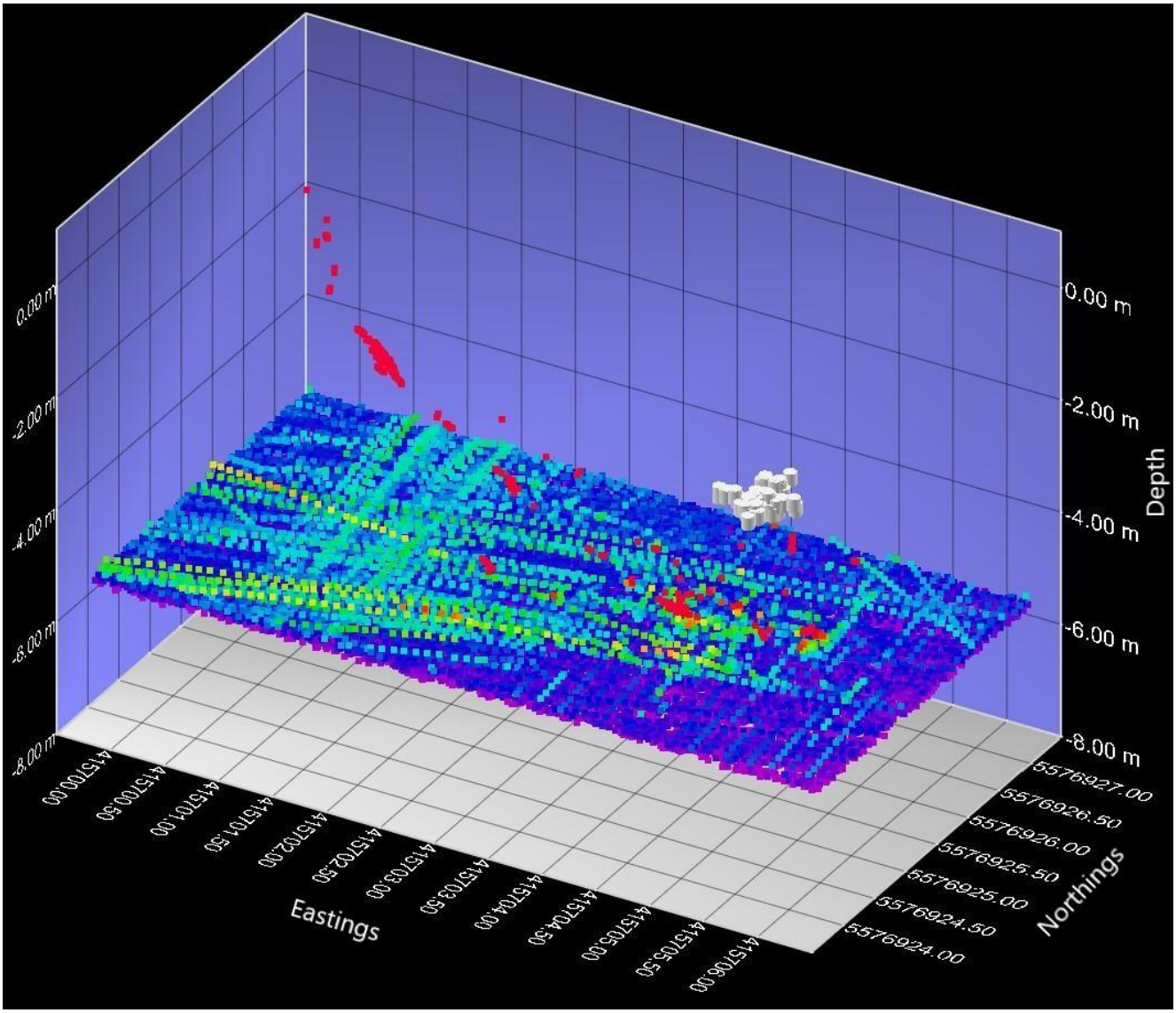

Figure 14. MBES filtered data of the mid-water target.

5.0 Discussion

5.1 3DSS-IDX-450 (CAATI and MBES Engine)

Interferometric sonars for shallow water hydrography (e.g. (Kraeutner and Bird, 1999; Lurton, 2000; Czotter *et al.*, 2016) have evolved in recent years with the development and incorporation of advanced technologies (e.g., Brissette *et al.*, 1997; Singh *et al.*, 2019; Grall *et al.*, 2020) to obtain high accuracy imaging and bathymetric data. Robust tests evaluated the bathymetric and object detection performance of the 3DSS-IDX-450 Sonar of Ping DSP with integrated CAATI and MBES engine to determine its ability against industry-grade MBES. The 3DSS-IDX-450 combined accurate wide swath bathymetry with high-resolution dual-frequency 3D (and 2D) imagery for complete hydrographic and imaging solutions (Brisson *et al.*, 2014) to meet IHO Standards (Order 1 Special order). Ping DSP patented Computed Angle-of-Arrival Transient Imaging (CAATI) employed by the 3DSS-IDX-450 used multi-channel phased transducer arrays with signal processing procedures to resolve multiple simultaneous backscatters in real-time. Kraeutner and Bird, 1999 described the CAATI technique as efficient in significantly minimising multipath interference, which traditional interferometric systems lack. The MBES Bathymetry Engine used an advanced seafloor detection algorithm to provide
accurate, wide swath bathymetry using the dual head nature of 3DSS Sonar and its high-resolution 3D imaging capability (Ping DSP Inc, 2018a). The combined techniques of CAATI and MBES Bathymety Engine allowed the water column target to be resolved independent of seabed backscatter producing actual 3D side scan imagery and bathymetry compliant with IHO Order 1 and Special Order. The test results demonstrated the bathymetric and object detection capability of the 3DSS-IDX-450 to meet IHO Order 1a&b and Special Order (TVU of 0.11m (95% c.l.)). Pulse footprint soundings based on the CAATI algorithm provided a high-resolution profile of the seabed and fine-scale features. The pulse footprints were combined to produce soundings from larger footprints with increased noise immunity, thereby improving the quality of the seabed data acquired (e.g., Kraeutner, 1998; Li *et al.*, 2007).

5.2 Object detection

5.2.1 Seabed Target

Utilising the CAATI algorithm, each backscatter arrival was given a range and angle value relative to the sonar head. These raw data points were then visualised in a point cloud display, resulting in a geometrically correct 3D of seabed targets. This capability allowed for complete resolution imaging and accurate representation of the imaged target with intuitive user manipulation of the data (Dragun *et al.*, 2017). Sample images of the same seabed target (0.5m cube) taken with Norbit iWBMS and 3DSS-IDX-450 Sonar as a 3D point cloud with the colour of the points scaled by the backscatter intensity are shown in figure 12. Due to differences in imaging geometry of both systems (Norbit at 1m altitude and Ping DSP at 30cm below the water surface), their frequencies and beamwidths ((400kHz, 0.5º horizontal by 55º vertical for Norbit and 450kHz, 0.5º horizontal by 65º vertical for Ping DSP) were optimised to produce similar quality imagery of the seabed target. The cube in the CAATI filtered 3D point cloud data from the 3DSS-IDX-450 Sonar was readily detectable and differentiable in shape and dimension, same as in the Norbit iWBMS image with similar sharpness. The Norbit image has a sharper

focus. However, the 3D side scan data had reduced sharpness and blurring of the image features on the seabed resulting from the intensity of the signal from the water column (Hayes and Barclay, 2003). The region in the 3D point cloud beneath the target showed elevated inconsistency in the depth of the identified seabed, as some points fell below the seabed. This is probably an effect of the intense highlight from the target when processing the phase data for the rest of the samples in those pings (e.g., Crawford and Connors, 2018). The design of the CAATI algorithm was meant explicitly to reduce the impact of multipath interference on background noise. During the Ping DSP sonar testing, part of the attempt was characterising the system background noise on the USV platform, contributing to a marginally elevated background noise level. The Ping DSP Sonar's strength is its ability to image in three dimensions, which is illustrated in the hits on the target at each pass in table 3 & 5 and figure 12.

5.2.2 Midwater Target

The key objective of the test was to evaluate the performance of the 3dSS-IDX-450 Sonar in detecting fixed targets in midwater. Pairing highlights with shadows, locating anchors on the seafloor, and understanding imaging geometry constraints were the cues to detect the midwater target in the 3DSS sonar images (e.g., Midtgaard *et al.*, 2007). The water column signal returns were recognisable as the moored target on each pass (100% detection). The point cloud from all the passes by the 3m depth moored object (0.65m) with colour scaled by relative depth and backscatter signal level are shown in figures 13 and 14. The backscattered intensity of the target highlight was a much less dependable indicator than the presence of the three-dimensional shape in midwater, including the hits on the mooring cable of the anchorage. The trial of the 3dSS-IDX-450 Sonar has demonstrated its ability to meet the requirements of IHO object detection Order 1 and Special Order (IHO, 2020) (1m cube of object projecting above the seafloor) (Kraeutner *et al.*, 2002; Crawford and Connors, 2018). As a result of suitable object-sonar geometry, relative to the transmit and receive beam patterns and the sonar transmit pulse, there was enough hits on the midwater target (Figure 13 & 14).

6.0 Conclusion

6.1 Bathymetry

The 3DSS sonar (a Multi-angle Swath Bathymetry Sidescan (MSBS)) produces bathymetric soundings comparable to an ideal multibeam sonar without sidelobes, beam spreading, or asymmetrical beam sensitivity inherent in traditional beam steering systems. Quantitative bathymetric analysis of 3DSS-IDX-450 Sonar compared to Norbit iWBMS using a reference surface survey and bathymetric uncertainty tests in shallow water was presented in this study. The Ping DSP's 3DSS- IDX-450 Sonar has demonstrated its ability to meet the TVU and THU standards of IHO Order 1 and Special Order (within 20º-140º swath). The patented CAATI and 3DSS MBES engine have been seen to overcome many of the limitations inherent in traditional interferometric systems, achieving an overall depth uncertainty of 0.110m (95% c.l.) compared to Norbit iWBMS with 0.042m on a shallow seabed with a steady slope to death of 6.5m. The variability of the bathymetry is decreased using CAATI due to the inherent separation of the seabed backscatter arrivals and concurrent multipath interference. 3DSS soundings were each obtained from an individual range sample instead of multiple range samples within a beam of multibeam echo sounders. This technique delivers high-sounding densities and 3D imagery together with bathymetric data. Since the Ping DSP, through its CAATI technology, resolves multiple

simultaneous backscatter arrivals in real-time, a comparative study on its backscatter is suggested for investigation.

6.2 Object Detection

During this testing, the 3D side scan sonar could effectively detect seabed targets in shallow water (2 – 6.5m depth below CD). Based on their highlights, all seabed objects within the study area were identifiable and distinguishable. The CAATI design provided low shadow signal levels in areas with multipath existence for the MBES data, allowing the seabed target to be identified. However, in the 3D data, the seabed target could not be identified due to the inability of the Qimera software (third-party software used) to filter out the water column data and noise. The 3DSS-IDX-450 Sonar was highly efficient (100%) in distinguishing the midwater target, including the mooring cable and the anchor, which is one of its primary capabilities. At the same frequency, the targets were boxed-in at 0m, 10, and 20m (at both port and starboard). Further testing is recommended to detect the targets at different frequencies. The three-dimensional point clouds on the midwater target were geometrically reliable with the actual target shape and dimensions. With enough hits on the target, there is an excellent opportunity for successful detection processing using deep learning and artificial intelligence.

References

Brissette, M. B., Hughes-Clarke, J. E., Bradford J. and MacGowan, B. (1997) 'Detecting small seabed targets using a high frequency multibeam sonar: Geometric models and test results', *Oceans Conference Record (IEEE)*, 2, pp. 815–819. doi:10.1109/oceans.1997.624099.

Brisson, L. N., Wolfe, D. A. and Staley, M. P. (2014) 'Interferometric Swath Bathymetry for Large Scale Shallow Water Hydrographic Surveys', in *Canadian Hydrographic Conference*, pp. 1–18.

Bu, X., Mei, S., Yang, F., Luan, Z., Xu, F. and Luo, Y. (2021) 'A Precise Method to Calibrate Dynamic Integration Errors in Shallow- and Deep- Water Multibeam Bathymetric Data', *IEEE Transactions on Geoscience and Remote Sensing*. IEEE, pp. 1–14. doi: 10.1109/TGRS.2021.3097723.

Crawford, A. and Connors, W. (2018) 'Performance Evaluation of a 3-D Sidescan Sonar for Mine Countermeasures', *IEEE Xplore*. IEEE, pp. 1–6. doi: 10.1109/OCEANS.2018.8604811.

Crawford, A. and Connors, W. (2019) 'Performance Evaluation of a 3-D Sidescan Sonar for Mine Countermeasures', *OCEANS 2018 MTS/IEEE Charleston, OCEAN 2018*. IEEE, pp. 1–6. doi: 10.1109/OCEANS.2018.8604811.

Czotter, K., Kraeutner, P. and Jackson, D. (2016) 'Shallow water surveying with swath bathymetry 3D sidescan Kalman', in *Canadian Hydrographic Conference*, p. 1.

Dando, P. R. (1975) 'On the northern rockling ciliata septentrionalis (collett) in the plymouth area', *Journal of the Marine Biological Association of the United Kingdom*, 55(4), pp. 925–931. doi: 10.1017/S002531540001780X.

Dragun, D., Noppe, L., Serpe, P., Caron. E. and Robert, A. (2017) 'Semi-Buried Seabed Object Detection: Sonar vs. Geophysical Methods', in *FIG Working Week 2017*.

Fakiris, E. *et al.* (2019) 'Multi-frequency, multi-sonar mapping of shallow habitats-efficacy and management implications in the National Marine Park of Zakynthos, Greece', *Remote Sensing*, 11(4). doi: 10.3390/rs11040461.

Geen, M. (1998) 'Applications of interferometric swath bathymetry', *Oceans Conference Record (IEEE)*, 40(6), pp. 1126–1130. doi: 10.1109/oceans.1998.724411.

Gibbs, P. E. (1969) 'A quantitative study of the polychaete fauna of certain fine deposits in Plymouth Sound', *Journal of the Marine Biological Association of the United Kingdom*, 49(2), pp. 311–326. doi: 10.1017/S0025315400035931.

Grall, P., Kochanska, I. and Marszal, J. (2020) 'Direction-of-arrival estimation methods in interferometric echo sounding', *Sensors (Switzerland)*, 20(12), pp. 1–17. doi: 10.3390/s20123556.

Hayes, M. and Barclay, P. (2003) 'The effects of multipath on a bathymetric synthetic aperture sonar using belief propagation', *Proc. Image and Vision Computing New Zealand (IVCNZ2003)*, (1), pp. 66–71.

IHO (2020) 'International Hydrographic Organization Standards for Hydrographic Surveys S-44', *International Hydrographic Organization*, (377), p. 49. Available at: www.iho.int.

IMCA (2015) *Guidelines for The Use of Multibeam Echosounders for Offshore*. Swindon, U.K. Available at: www.imca-int.com.

Kendall, M. A. and Widdicombe, S. (1999) 'Small scale patterns in the structure of macrofaunal assemblages of shallow soft sediments', *Journal of Experimental Marine Biology and Ecology*, 237(1), pp. 127–140. doi: 10.1016/S0022-0981(98)00224-X.

Kenny, A. J., Cato, I., Desprez, M., Fader, G., Schu¨ttenhelm, R. T. E. and Side, J. (2003) 'An overview of seabed-mapping technologies in the context of marine habitat classification', *ICES Journal of Marine Science*, 60(2), pp. 411–418. doi: 10.1016/S1054-3139(03)00006-7.

Kraeutner, P. H. (1998) *Small Aperture Acoustic Imaging using Mode1 Based Array Signal Processing*. SIMON FRASER UNIVERSITY. Available at: https://central.bac-lac.gc.ca/.item?id=NQ37723&op=pdf&app=Library&is_thesis=1&oclc_number=46907787.

Kraeutner, P. H. *et al.* (2002) 'Multi-angle swath bathymetry sidescan quantitative performance analysis', *Oceans Conference Record (IEEE)*, 4, pp. 2253–2263. doi: 10.1109/oceans.2002.1191981.

Kraeutner, P. H. and Bird, J. S. (1999) 'Beyond Interferometry, Resolving Multiple Angles-of- Arrival in Swath Bathymetric Imaging', *IEEE Journal of Oceanic Engineering*, pp. 37–45. Available at: https://ieeexplore.ieee.org/stamp/stamp.jsp?tp=&arnumber=799704.

Leenhardt, O. (1974) 'Side Scanning Sonar - A Theoretical Study', *The International Hydrographic Review*, 50(1–2), pp. 61–80.

Li, Z. S. *et al.* (2007) 'Multiple sub-array beamspace CAATI algorithm for multibeam bathymetry system', *Journal of Marine Science and Application*, 6(1), pp. 47–52. doi: 10.1007/s11804-007-6020-x.

Lurton, X. (2000) 'Swath bathymetry using phase difference: theoretical analysis of acoustical measurement precision', *IEEE Journal of Oceanic Engineering*, 25(3), pp. 351–363. doi: 10.1109/48.855385.

Midtgaard, Ø., Sæbø, T. O. and Callow, H. J. (2007) 'Detection of short-tethered objects with interferometric synthetic aperture sonar', *Oceans Conference Record (IEEE)*. doi: 10.1109/OCEANS.2007.4449366.

NORBIT, S. (2022) *NORBIT - iWBMS TURNKEY MULTIBEAM SONAR SYSTEM*. PS-120006-23. Trondheim, Norway. Available at: https://norbit.com/media/PS-120006-23_iWBMS_Pn_12004_AACDB4_A4.pdf.

Parry, D. M. *et al.* (1999) 'Species body size distribution patterns of marine benthic macrofauna assemblages from contrasting sediment types David', *Journal of the Marine Biological Association of the United Kingdom*, 94(14), pp. 5077–5078. doi: 10.1021/ja00769a048.

Ping DSP Inc. (2017) *3DSS TM MBES Bathymetry Engine*. Available at: http://www.pingdsp.com/pdf/MBES Bathymetry Engine.pdf (Accessed: 20th December 2021).

Ping DSP Inc. (2020) '3DSS-DX and 3DSS-iDX Sonar Manual'. North Saanich, British Columbia, Canada: U.S. Patent (2.1). Available at: www.pingdsp.com.

Ping DSP Inc (2018a) *3DSS Sonar Data Example: Bathymetry in the Presence of Water Column Targets*. Available at: www.pingdsp.com (Accessed: 20th December 2021).

Ping DSP Inc (2018b) *INNOVATION IN MINE DETECTION*. Available at: www.pingdsp.com (Accessed: 20th December 2021).

Saunders, J. E. *et al.* (2003) 'Spatial variability in the epiphytic algal assemblages of Zostera marina seagrass beds', *MARINE ECOLOGY*, 249, pp. 107–115.

Shang, X., Zhao, J. and Zhang, H. (2019) 'Obtaining high-resolution seabed topography and surface details by Co-Registration of side-scan sonar and multibeam echo sounder images', *Remote Sensing*, 11(12), pp. 1–21. doi: 10.3390/rs11121496.

Singh, J., Ioana, C., Geen, M. and Mars, J. (2019) 'Interferometric Measurements with Wideband Signal Processing Techniques',
IEEE. doi: 10.1109/OCEANSE.2019.8867232.

BIOGRAPHICAL NOTES

Sebastian Botsyo is the officer in charge of hydrography at the Survey and Mapping Division, Lands Commission – Ghana and a lecturer in hydrographic surveying, land surveying principles and remote sensing at the Ghana School Surveying and Mapping. A resourceful person with a technical background in Geomatic Engineering, Hydrography, and GIS and have the potential for world-leading research and teaching in any aspect of Land Surveying, Hydrography, Ocean, and Geospatial Engineering. Sebastian have more than 15 years of experience in the collection and analysis of coastal morphological (coastal erosion and protection), coastal sediment transport processes and hydrographic data. My academic research has resulted in peer-reviewed international journal articles and conference papers, technical reports, invited lectures, workshops and seminars. In addition to academic research, He has conducted several consultancy projects.

Mr. Botsyo obtained MSc in Hydrography (Cat A) at the University of Plymouth, UK in November 2022. Prior to his study in hydrography, he obtained MPhil in GIS (2019) and BSc in Geomatics Engineering (2016) all from the Kwame Nkrumah University of Science and Technology, Kumasi, Ghana. He also studied Surveying and Mapping at the Ghana School of Surveying and Mapping (GSSM) in Accra (2006) and pursued Geo-Informatics (GIS Operations) at, the University of Twente, Netherlands (2012). He studied basic education at St. Francis Teacher Training College in Hohoe from 1999 to 2002 to obtain Teachers Certificate 'A'.

He is a professional member of the Ghana Institution of Surveyors (GhIS), American Geophysical Union (AGU), Hydrographic Society UK – Student/New Graduate member, Young Surveyors Network, FIG. Also, a student member of RICS, IES, CICES and IMarEST.

CONTACTS

Title Given name and family name: Sebastian Senyo Botsyo
Organisation: Survey and Mapping Division, Lands Commission
Address: P.O. Box CT903
City: Accra
Country: Ghana
Tel. +233243171027
Email: kwasisesebot@gmail.com
Web site: www.lc.gov.gh